Research Journal of Applied Sciences, Engineering and Technology 6(7): 1153-1159, 2013
DOI:10.19026/rjaset.6.3925
ISSN: 2040-7459; e-ISSN: 2040-7467

Submitted: June 30, 2012 Accepted: July 26, 2012 Published: July 05, 2013

Research Article

A Finger Vein Recognition Method Using Improved Oriented Filter and Elastic Registration

[1]Ma Hui, [2]Popoola Oluwatoyin P. and [1]Sun Shuli
[1]College of Electronic Engineering, Heilongjiang University, Harbin 150001, China
[2]Systems Engineering Department, Faculty of Engineering, University of Lagos, Akoka, Nigeria

Abstract: In order to reduce the influence of relative position deviation and angle deviation between minutia point sets caused by external factors when finger vein images are obtained, a finger vein recognition method using elastic registration is presented. The proposed algorithm is based on an improved neighborhood direction template and oriented filter template which facilitates the enhancement of the finger vein image while taking full account of image orientation. Elastic registration is then applied to matching of feature points within the predefined angle and radius. Applying the idea of elastic registration to existing finger vein recognition method removes the need for perfect matching between corresponding feature points and has shown to be an effective method for dealing with the problem of nonlinear distortion of images. Experimental results show that this algorithm not only overcomes the limitations of traditional point matching method, but also effectively improves the recognition performance of the system.

Keywords: Elastic registration, finger vein recognition, improved oriented filter, minutia point feature

INTRODUCTION

Finger vein image recognition makes use of short near infrared transmission on the finger to obtain vein features for personal identification. It is a very reliable biometric recognition method with the merits of being rapid, precise and non-contact. The human vein network structure extends to body extremities like fingers and toes. Research has shown that the vein patterns in body parts of individuals are distinct and remarkably different. This makes finger vein image recognition a choice method in biometric recognition (Kumar and Prathyusha, 2010; Kang *et al*., 2011).

There are currently many finger vein image recognition methods which adopt local features to describe finger vein details. Lin *et al*. (2003) proposed a vein recognition method based on feature points matching. Results show that this algorithm has accurate identification but time intensive. Miura *et al*. (2004) proposed a finger vein feature extraction method based on repeat alignment tracking. Ladoux *et al*. (2009) on the other hand, used SIFT (Scale Invariant Feature Transform) corner detection as feature points for performing recognition. Badawi (2006) proposed a vein recognition method based on pixel matching while Wang and Leedham (2007) used of finger vein cross-over points as feature points to do recognition. A feature point recognition method is used in Lee and Park (2009), which is based on endpoints of the finger vein. These afore mentioned algorithms adopt minutia point features of the vein to complete finger vein image matching. The methods perform well with good results in either speed or recognition, but their recognition results are easily influenced by image quality; causing high false reject and false accept rates during the matching process. Apart from these local feature recognition methods, there is also global feature recognition methods. Wang and Yuan (2007) proposed a finger vein recognition method based on wavelet moment by fusing it with PCA and LDA transform. Jia *et al*. (2011) adopted Contour let moment to accomplish the global matching task for finger vein image. Wang *et al*. (2008) likewise, proposed a finger vein recognition method based on Laplace transform. Compared with the local feature recognition methods, global feature recognition methods make full use of finger vein information, but their recognition results also get affected negatively in the presence of rotation and translation in finger vein images. In view of the above mentioned problems relating to the existing algorithm and the characteristics of vein images, a new finger vein recognition method with improved oriented filter and elastic registration was studied. The proposed algorithm is based on an improved neighborhood direction template and oriented filter template which facilitates the enhancement of the finger vein image taking into full account of image orientation. On this basis, we apply elastic registration to recognize finger vein minutia point features. Computation burden is

Corresponding Author: Ma Hui, College of Electronic Engineering, Heilongjiang University, Harbin 150001, China

minimized using this feature point method as there is no need to extract all characteristic information from the finger vein image. The proposed method is also able to overcome the problem of noise and geometrical distortion of an image since there is no need for one-to-one correspondence between the feature point sets of any two images. Experimental results show that this algorithm not only overcomes the limitations of traditional point matching methods, but also effectively improves the recognition performance of the system.

Finger vein image preprocessing: If the quality of pre-processed image is poor there will be false feature points in the course of feature extraction which can dramatically degrade the system performance. The recognition rate achieved by matching methods using minutia points feature sets is closely linked with image quality. Therefore there is the need for a series of image preprocessing operations on original finger vein images in order to remove redundant information and accurately obtain the feature points set.

Finger region extraction: Environmental factors have a great influence on image acquisition. This becomes evident as the gray values of background pixels don't all have the desired '0'. In order to limit background effect on feature extraction and recognition, we need to identify finger region pixels before extracting finger vein features.

Further isolation of the finger region was completed using the Kapur entropy threshold algorithm. Burrs in the segmented image are removed using the open operation of mathematical morphology. Figure 1 shows some experimental results of the vein image region extraction process.

Orientation filter enhancements: As can be seen from the topology of the finger vein image, finger veins have marked directionality characteristics. They also extend in a particular direction. Traditional filter methods do not take into account the directionality characteristics of the finger vein; therefore its resultant filtering enhancement is not satisfactory. We use oriented filtering technology to enhance finger vein image in accordance with the directionality feature of the veins. Our algorithm utilizes a group of oriented filters to filter the image depending on pixel orientation.

To estimate the orientation field of vein image, the direction of the vein is divided into eight

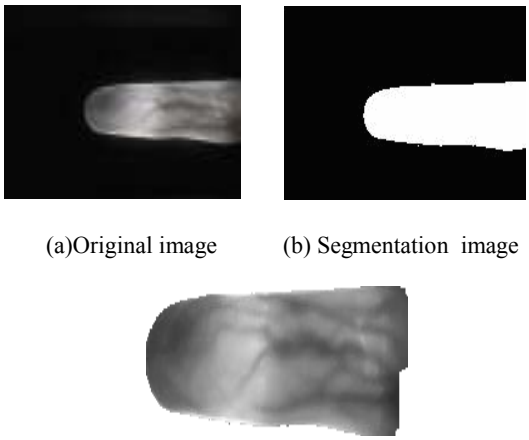

(a)Original image (b) Segmentation image

(c) Finger region image

Fig. 1: Finger vein image region extraction process

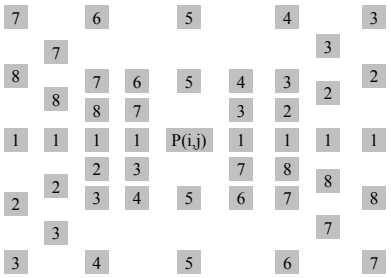

(a) 9×9 neighborhood template

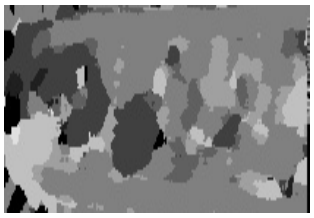

(b) A directional image of finger vein

Fig. 2: Neighborhood template image and directional image

directions. Using a 9*9 neighborhood-template window as shown in Fig. 2a, a reference pixel $p(i, j)$ is chosen as the center of the direction template. Eight different directions (values 1-8) of the template are range from 0 to π in an anti-clockwise direction from the horizontal axis, each having an interval angle of $\pi/8$. There are more neighborhood-pixels tending in the horizontal direction namely directions 1, 2, 3, 7 and 8, while there are fewer in the vertical direction such as 4, 5 and 6. This is a suitable template for finger vein image.

The pixel direction can be determined by the assumption that pixels along the vein ridge have

minimum gray level difference whereas pixels that are perpendicular to the vein ridge have maximum gray level difference. To establish this, the above neighborhood-template was used to obtain every pixel gray values' average $\bar{G}_1(l = , \ldots, 8)$. First, divide $\bar{G}_1$ into four groups. $\bar{G}_1$ and $\bar{G}_5$ are perpendicular in direction, so they belong to the same group. In the same token, $\bar{G}_2$ and $\bar{G}_6$, $\bar{G}_3$ and $\bar{G}_7$, $\bar{G}_4$ and $\bar{G}_s$ belong to the same group. Then calculate ΔG as the absolute difference between two gray value averages $\bar{G}_j$and $\overline{G_{J+4}}$ in each group. ΔG is defined as:

$$\Delta G_k = \left| \overline{G_k} - \overline{G_{k+4}} \right| \quad (1)$$

where k is the direction of the vein (k = 1, 2, 3, 4). Choose the maximum ΔG_k to determine the pixel's possible directions k_{max} and k_{max} +4. Determine the actual direction of p(i, j) by comparing its gray value with the gray value averages of k_{max} and k_{max} +4. The closer value is its direction. Therefore the pixels direction D(x, y) is given by:

$$D(x,y) = \begin{cases} k_{\max}, if \left| G - \overline{G}_k \right| < \left| G - \overline{G}_k + 4 \right| \\ k_{\max} + 4, otherwise \end{cases} \quad (2)$$

The directional image D(x, y) of the vein image is determined when the above stated process is performed on each image pixel. However, because of the presence of noise in the vein image however, often makes the estimated orientation field incorrect. Pixels' orientations are generally uniform in a small local neighborhood and so a local ridge orientation is specified for a block rather than per pixel. Some experimental results can be seen in Fig. 2b. Eight filter masks were designed; each one associated with the discrete ridge orientation of the finger vein pixels. Using O'Gorman's rules for filter design of fingerprint images enhancement, we modify the filters' coefficients based on direction such that there is a decaying effect from the center to both ends of the template. The template coefficients of horizontal mask is first determined and then the other 7 masks are generated by rotating the horizontal filter mask according to the vein direction. Template overlap occurs when the horizontal filter template is rotated. Therefore the filter template of size 7 was expanded to size 9. The expanded horizontal filter template is shown in Fig. 3a with the outermost row and column coefficients all zero. Positions that have no coefficients in the rotated template are represented by zero. The rotated template is shown in Fig. 3b. It avoids the template overflow problem which occurs when the horizontal filter template is rotated, while keeping a balance in the coefficient distribution. Once we have got all 8 filter masks, their coefficients can be used to enhance the vein image.

0	0	0	0	0	0	0	0	0
0	-c/3	-2c/3	-c	-c	-c	-2c/3	-c/3	0
0	b/3	2b/3	b	b	b	2b/3	b/3	0
0	a/3	2a/3	a	a	a	2a/3	a/3	0
0	d/3	2d/3	d	d	d	2d/3	d/3	0
0	a/3	2a/3	a	a	a	2a/3	a/3	0
0	b/3	2b/3	b	b	b	2b/3	b/3	0
0	-c/3	-2c/3	-c	-c	-c	-2c/3	-c/3	0
0	0	0	0	0	0	0	0	0

(a) Template of horizontal oriented filter

0	0	0	0	0	-2c/3	-c/3	0	0
0	0	0	-c	-c	2b/3	b/3	0	0
-c/3	-2c/3	-c	b	b	2a/3	a	0	0
b/3	2b/3	b	a	a	a	2d/3	d	0
0	a/3	2a/3	d	d	d	2a/3	a/3	0
0	d/3	2d/3	a	a	a	b	2b/3	b/3
0	0	a/3	2a/3	b	b	-c	-2c/3	-c/3
0	0	b/3	2b/3	-c	-c	0	0	0
0	0	-c/3	-2c/3	0	0	0	0	0

(b) Template of the rotated oriented filter

Fig. 3: 9×9 rectangular window

Fig. 4: Image enhanced by oriented filter

The corresponding direction filter is selected from a series of filters, to filter the image area according to the direction feature of the image area. An enhanced image is shown in Fig. 4.

Feature point extraction: One simple and yet effective method of segmentation is the local dynamic threshold algorithm proposed by NiBlack; and this was used in our image segmentation step. Thinning operation is performed on the segmented vein image in order to enable further data compression. An 8-neighborhood feature point extraction algorithm is used to extract end points and crossing points after the thinning operation. Experimental results can be seen in Fig. 5a. Figure

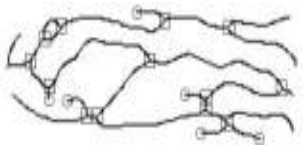

(a) Oriented filter and Niblack

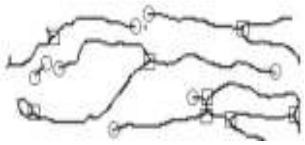

(b) Only Niblack

Fig. 5: Image of minutiae feature

5b is the result without using improved oriented filter. There are a few pseudo-vein characteristics in Fig. 5b. This results in missing important feature points or extracting false feature points during the feature points' extraction process. In contrast, the vein is smooth and continuous in Fig. 5a. The feature points extracted from this kind of image are very accurate and this buttresses the validity of our improved oriented filter method.

Finger vein image recognition:

Point pattern matching principle: Suppose the feature point set for finger vein image is given by P = {p_1, p_2, ...,p_m} and the input image feature point set is Q = {q_1, q_2, ..., q_n}. Matching operation between any two minutia point feature sets uses a calibration function G(t_x, t_y, s, θ) to get G(p_i) = qi. There are four parameters in this calibration function namely: t_x ,t_x , denoting the displacement of template image and matching image in the *x* and *y* directions respectively. The parameter s represents the compounding coefficient between template image and input image, while θ is the value of angular difference between template image and matching image.

Feature points of set *P* and set *Q* can represent by *X* and *Y* co-ordinates as follows:

$$P = \{(x_{p_i}, y_{p_i})^T \Big| , i = 1 \cdots\cdots m\} \tag{3}$$

$$Q = \{(x_{q_j}, y_{q_j})^T \Big| , j = 1 \cdots\cdots n\} \tag{4}$$

There exists only one corresponding relationship in set P and set Q, then $Q = G(p)$ the formula can be expressed as:

$$\begin{pmatrix} x_q \\ y_q \end{pmatrix} = \begin{pmatrix} t_x \\ t_y \end{pmatrix} + \begin{pmatrix} s\cos(\theta) & -s\sin(\theta) \\ s\sin(\theta) & s\cos(\theta) \end{pmatrix} \begin{pmatrix} x_p \\ y_p \end{pmatrix} \tag{5}$$

It can be seen from formula (5) that the calibration function has multiple solutions. If there are two points p_i, p_a in set *P* and two points q_i, q_a in set *Q* having corresponding relationships .and if $p_i \neq p_a$ and $q_j \neq q_b$,then there exists only one calibration function G(t_x, t_y, s, θ) which is used to match set *P* and set *Q*, that is

$$G(p_i) = q_j,\ G(p_a) = q_b .$$

where,

$$s = \frac{|q_j q_b|}{|p_i p_a|} \tag{6}$$

$$\theta = \theta_{q_j q_b} - \theta_{p_i p_a} \tag{7}$$

$$t_x = x_{q_j} - x_{p_i}(s\cos\theta) + y_{p_i}(s\sin\theta) \tag{8}$$

$$t_y = y_{q_j} - x_{p_i}(s\cos\theta) + y_{p_i}(s\cos\theta) \tag{9}$$

because $G(p_i) = q_j,\ G(p_a) = q_b .$

Expanding respectively gives:

$$\begin{pmatrix} x_{q_j} \\ y_{q_j} \end{pmatrix} = \begin{pmatrix} t_x \\ t_y \end{pmatrix} + \begin{pmatrix} s\cos(\theta) & -s\sin(\theta) \\ s\sin(\theta) & s\cos(\theta) \end{pmatrix} \begin{pmatrix} x_{p_i} \\ y_{p_i} \end{pmatrix} \tag{10}$$

$$\begin{pmatrix} x_{q_b} \\ y_{q_b} \end{pmatrix} = \begin{pmatrix} t_x \\ t_y \end{pmatrix} + \begin{pmatrix} s\cos(\theta) & -s\sin(\theta) \\ s\sin(\theta) & s\cos(\theta) \end{pmatrix} \begin{pmatrix} x_{p_a} \\ y_{p_a} \end{pmatrix} \tag{11}$$

(11)- (10) is:

$$\begin{pmatrix} x_{q_b} - x_{q_j} \\ y_{q_b} - y_{q_j} \end{pmatrix} = \begin{pmatrix} 0 \\ 0 \end{pmatrix} + \begin{pmatrix} s\cos(\theta) & -s\sin(\theta) \\ s\sin(\theta) & s\cos(\theta) \end{pmatrix} \times \begin{pmatrix} x_{p_a} - x_{p_i} \\ y_{p_a} - y_{p_i} \end{pmatrix} \tag{12}$$

Make $q_j q_b = \begin{pmatrix} x_{q_b} - x_{q_j} \\ y_{q_b} - y_{q_j} \end{pmatrix}$ $p_i p_a = \begin{pmatrix} x_{p_a} - x_{p_i} \\ y_{p_a} - y_{p_i} \end{pmatrix}$, then:

$$q_j q_b = \begin{pmatrix} 0 \\ 0 \end{pmatrix} + \begin{pmatrix} s\cos(\theta) & -s\sin(\theta) \\ s\sin(\theta) & s\cos(\theta) \end{pmatrix} p_i p_a \tag{13}$$

It can be seen from formula (13) that there exist a new calibration function G (0, 0, s, θ) that makes $p_i p_a$ and $q_j q_b$ have corresponding relationships. That is:

$$G(p_i p_a) = q_j q_b \tag{14}$$

The four parameters of the calibration function can now be reduced to two parameters *s* and θ.

Finger vein image elastic registration recognition method: The preceding section was a presentation of matching between two feature point sets. But in practical applications, finger vein images are (in the image capture stage) easily influenced by noise factors due to illumination or positioning and this leads to matching of feature points with inherent deviations in position and angle, which negatively impacts recognition rate. To deal with this problem, an elastic registration approach is used in this study to achieve accurate matching of different finger vein minutia feature point sets. Our method also performs well because of the ability to overcome limitations of noise and geometrical distortion of image because there is no need for a one-to-one correspondence matching between feature point sets of any two images. When the deviation of corresponding points' position and angle in the two images is less than the given threshold, the two images are considered as matching.

Feature point matching means the matching of feature point's topological structure. If the feature point's topological structure of the template image and that of the matching image are approximately the same, we can think both images are matching. Otherwise, we conclude they don't match. Thus a similarity function can be defined as follows:

$$S = 4 \times M \times \frac{F_m}{F_t \times F_t} \tag{15}$$

where, M denotes the successful matching count for a feature point of the template image and another feature point of the input image. If there is a match between the template image and input image, the value of M increases by one. F_t is the total number of feature points of the template and input images and F_m is the maximum number of matching feature points. If the similarity value is greater than the threshold, we consider the two finger vein images as matching.

The above-mentioned determines the similarity between feature points as follows: suppose P is one feature point of the template finger vein image and P' is one feature point of the input image. If P and P' are exactly the same, then P = P'. In practice however, because of error factors P and P' are not exactly the same this can me mathematically described as P ≈ P' that is P = P' + Δ. Where Δ is the range of elastic registration.

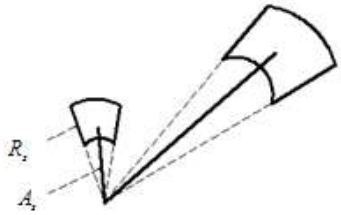

Fig. 6: Pictorial diagram of elastic range

The idea of elastic registration range means that there is an indeterminate area region around the feature point. This region consists of four sides having two sides as polar radius and the other two sides as polar angles. The difference in value between the two polar radii A_s denotes the width of elastic registration range and the difference in value between the two polar angles R_s denotes the height of the elastic registration range. Thus elastic registration range is determined by A_s and R_s .

The value of A_s and R_s varies with the polar radius of the feature point. If the polar radius of the feature point is large, then the value of R_s is also large and the value of A_s is small. There is variance in the value of Δ . A pictorial diagram of elastic range is shown as Fig. 6, where A_s means the angle of elastic registration range and R_s means the radius of elastic registration range.

When the polar radius of minutia point is equal tor, R_s is given by:

$$R_s = \begin{cases} R_{min}, & R < R_{min} \\ R, & R_{min} < R < R_{\max} \\ R_{\max}, & R > R_{\max} \end{cases} \tag{16}$$

$$R = \frac{r}{a} \tag{17}$$

When the polar radius of minutia point is equal to r, A_s is given by:

$$A_s = \begin{cases} A_{\min}, & A < A_{\min} \\ A, & A_{\min} < A < A_{\max} \\ A_{\max}, & A < A_{\max} \end{cases} \tag{18}$$

$$A = \frac{\beta}{r^2} \tag{19}$$

where, R_{min}、R_{max}、A_{min}、A_{max} is the upper bounds and lower bounds on R_s and A, α and β are constant.

The overall procedure of our method is as follows:

- Determine whether template feature point P matches with feature point p such that as $P \approx P'$. If the assumption fails, compare another pair of feature points otherwise turn to step 2 until all feature points matching is complete, then proceed to the last step.
- Accumulate the number of scores and similarity feature points.
- Calculate the matching similarity according to similarity formula, then compare its value with standard threshold to judge matching success is or not.

EXPERIMENTAL RESULTS

In order to verify the feasibility of the above-mentioned modeling method, we use an in-house collected database of 300 finger vein images. Each of the 300 persons had five forefinger vein images of size 320×240 captured and stored using the infra-red finger vein image capture device. A sample of images from our database is shown in Fig. 7.

Comparative analysis of results: To compare the performance of traditional feature point matching method (Wang and Leedham, 2007) and our method, we test both methods with 1:1 authentication experiment and 1: n recognition experiment. One finger vein image was chosen at random from five images of each person as the verification database and the others as the template database. The experimental results are shown in Table 1 and 2.

Experimental results indicate that our method not only has a higher recognition rate than the traditional feature point matching method, but also a lower false reject rate.

Rotation and translation test: Spatial variations take place during the finger vein image capture process. Images captured from the same finger have various degrees of translation and rotation at different times. Two experiments were designed to investigate the effects of translation and that of rotation on recognition rate. One finger vein image was chosen at random from five images of each person as the verification database and the others as the translation test database. Images from the original finger vein database were translated from one to five pixels to form the translation test database and also rotated from one to five degrees to form the rotation test database. The proposed method was tested using images of the translation test

Fig. 7: Some finger vein images from experimental database

Table 1: Results of three identification methods under 1:1 matching

Recognition mode	Matching times	FRR (%)
Method1	1200	13.7
Method2	1200	9.4
Our method	1200	5.8

Table 2: Results of three identification methods under 1: n recognition

Recognition mode	Matching times	# of accept	False far (%)
Method1	300	20	6.7
Method2	300	16	5.3
Our method	300	11	3.7

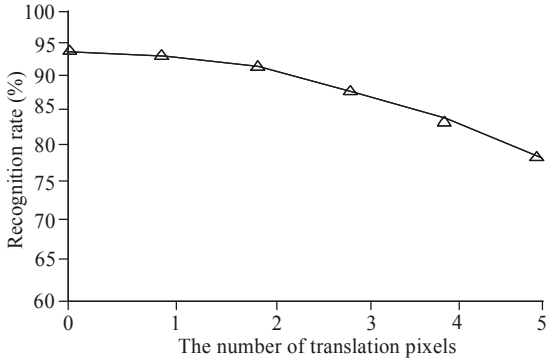

(a) Translation effect on recognition rate

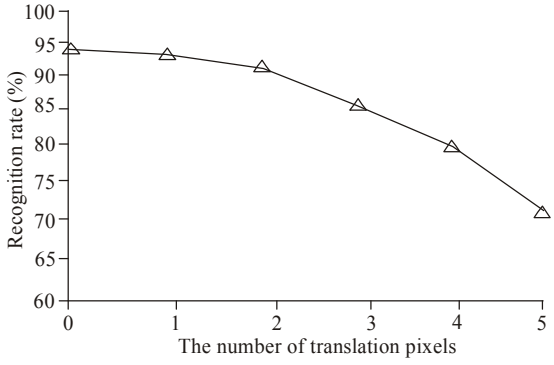

(b) Rotation effect on recognition rate

Fig. 8: Translation and rotation effect on recognition rate

database and rotation test database. The recognition results are shown in Fig. 8. Horizontal ordinate denotes the number of rotated pixels and vertical coordinates denotes the corresponding recognition rate of different translation pixels number or different rotation pixels number.

It can be seen from Fig. 8 that although there is gradual drop in the recognition rate for the translational image when the number of translation pixels varied from one to five pixels and for the rotational image when varying the rotation angle between one and four degrees, there is still a very significant recognition performance by the system (above 70%). This shows that the method is robust to the effects of translation and rotation- a very desirable property in real-life finger vein recognition systems.

CONCLUSION

In order to deal with the problem of finger vein image distortion, this study proposes a robust algorithm based on improved orientation filters and elastic registration. The algorithm extracts smooth and continuous vein image features enhanced by an improved oriented filter. This helps to obtain more accurate feature point sets. Then the algorithm makes effective use of local features of the finger vein image which greatly increases recognition rate. The elastic registration enhances the matching process, by not requiring a total correspondence between the entire feature points. When the deviation of corresponding points' position and angle in two images is less than the given threshold, both images are considered as matching. This method is also an effective for dealing with nonlinear image distortion. Experimental results indicate that it is robust to rotation and translation with a very significant improvement in recognition rates.

In future research, both local and global features of the finger vein image will be integrated to further improve the recognition rate. Further work will also be done to optimize algorithm and reduce the time consumed in the pre-processing operation in order to build a fast, accurate finger vein recognition system.

ACKNOWLEDGMENT

This study is partially supported by Science Fund for Young Scholars of Heilongjiang University (QL201111).

REFERENCES

Badawi, A.M., 2006. Hand vein biometric verification prototype: A testing performance and patterns similarity [C]. Proceeding of the International Conference on Image Processing, Computer Vision and Pattern Recognition. USA Press, Las Vegas, pp: 15-19.

Jia, X., X. Dingyu, C. Jian Jiang and L. Jing, 2011. Vein recognition based on fusing multi HMMs with contourlet sub-band energy observations [J]. J. Electron. Inform. Technol., 33(8): 1877-1882.

Kang, W., L. Huasong and D. Feiqi, 2011. Direct gray-scale extraction of topographic features for vein recognition [J]. Sci. Sin. Inform., 41(3): 324-337.

Kumar, A. and K.V. Prathyusha, 2010. Personal authentication using hand vein triangulation and knuckle shape [J]. IEEE T. Image Process., 9(18): 2127-2136.

Ladoux, P.O., C. Rosenberger and B. Dorizzi, 2009. Palm vein verification system based on SIFT matching [C]. Proceeding of 3rd International Conference on Advances in Biometric. Italy, pp: 1290-1298.

Lee, E.C. and K.R. Park, 2009. Restoration method of skin scattering blurred vein image for finger vein recognition [J]. Electron. Lett., 45(21): 1074-1076.

Lin, X.R., B. Zhuang and X.S. Su, 2003. Measurement and matching of human vein pattern characteristics [J]. J. Tsinghua Univ., Sci. Technol., 43(2): 164-167.

Miura, N., A. Nagasaka and T. Miyatake, 2004. Feature extraction of finger vein patterns based on repeated line tracking and its application to personal identification [J]. Mach. Vision Appl., 15(4): 194-203.

Wang, J.G., W.Y. Yau, S. Andy and E. Sung, 2008. Person recognition by fusing palmprint and palm vein images based on "Laplacian palm" representation [J]. Pattern Recogn., 41(5): 1514-1527.

Wang, K. and Z. Yuan, 2007. Finger vein recognition based on wavelet moment fused with PCA transform [J]. Pattern Recogn. Artif. Int., 20(5): 692- 697.

Wang, L. and G. Leedham, 2007. Infrared imaging of hand vein patterns for biometric purposes [J]. IET Comput. Vis., 1(3): 113-122.